



# Global Biogeochemical Cycles

## RESEARCH ARTICLE

10.1002/2013GB004637

### Key Points:

- Dissolved zinc biogeochemical cycle investigated in the South Atlantic Ocean

### Correspondence to:

N. J. Wyatt,  
neil.wyatt@plymouth.ac.uk

### Citation:

Wyatt, N. J., A. Milne, E. M. S. Woodward, A. P. Rees, T. J. Browning, H. A. Bouman, P. J. Worsfold, and M. C. Lohan (2014), Biogeochemical cycling of dissolved zinc along the GEOTRACES South Atlantic transect GA10 at 40°S, *Global Biogeochem. Cycles*, 28, 44–56, doi:10.1002/2013GB004637.

Received 19 APR 2013

Accepted 20 DEC 2013

Accepted article online 4 JAN 2014

Published online 27 JAN 2014

## Biogeochemical cycling of dissolved zinc along the GEOTRACES South Atlantic transect GA10 at 40°S

N. J. Wyatt<sup>1,2,3</sup>, A. Milne<sup>1,2</sup>, E. M. S. Woodward<sup>3</sup>, A. P. Rees<sup>3</sup>, T. J. Browning<sup>4</sup>, H. A. Bouman<sup>4</sup>, P. J. Worsfold<sup>1,2</sup>, and M. C. Lohan<sup>1,2</sup>

<sup>1</sup>Marine Institute, University of Plymouth, Plymouth, UK, <sup>2</sup>School of Geography, Earth, and Environmental Sciences, University of Plymouth, Plymouth, UK, <sup>3</sup>Plymouth Marine Laboratory, Plymouth, UK, <sup>4</sup>Department of Earth Sciences, University of Oxford, Oxford, UK

**Abstract** The biogeochemical cycle of zinc (Zn) in the South Atlantic, at 40°S, was investigated as part of the UK GEOTRACES program. To date there is little understanding of the supply of Zn, an essential requirement for phytoplankton growth, to this highly productive region. Vertical Zn profiles displayed nutrient-like distributions with distinct gradients associated with the water masses present. Surface Zn concentrations are among the lowest reported for the world's oceans (< 50 pM). A strong Zn-Si linear relationship was observed ( $Zn \text{ (nM)} = 0.065 \text{ Si } (\mu\text{M}), R^2 = 0.97, n = 460$ ). Our results suggest that the use of a global Zn-Si relationship would lead to an underestimation of dissolved Zn in deeper waters of the South Atlantic. By utilizing Si\* and a new tracer Zn\* our data indicate that the preferential removal of Zn in the Southern Ocean prevented a direct return path for dissolved Zn to the surface waters of the South Atlantic at 40°S and potentially the thermocline waters of the South Atlantic subtropical gyre. The importance of Zn for phytoplankton growth was evaluated using the Zn-soluble reactive phosphorus (SRP) relationship. We hypothesize that the low Zn concentrations in the South Atlantic may select for phytoplankton cells with a lower Zn requirement. In addition, a much deeper kink at ~500m in the Zn:SRP ratio was observed compared to other oceanic regions.

## 1. Introduction

Trace metal micronutrients such as zinc (Zn) play a key role in the productivity of the oceans. Zinc is an essential cofactor in many phytoplankton enzymatic processes [Vallee and Auld, 1990; Morel and Price, 2003] and as such is essential for phytoplankton growth. Zinc is used for the uptake of carbon dioxide (CO<sub>2</sub>) via the enzyme carbonic anhydrase [Morel et al., 1994; Tortell et al., 2000] and for organic phosphorus acquisition via the enzyme alkaline phosphatase [Shaked et al., 2006]. The vertical profile of Zn in the world's oceans resembles those of the major nutrients due to biological uptake and utilization [Bruland, 1980; Lohan et al., 2002; Ellwood, 2008; Croot et al., 2011; Jakuba et al., 2012]. As Zn is essential for phytoplankton growth, it has an impact on the global biological carbon pump. The stoichiometric relationship between Zn and the major nutrients, such as silicate and phosphate, is an important control on the efficiency and size of this pump.

In oceanic surface waters, Zn concentrations are < 0.1 nM with approximately 98% of this pool chelated by strong organic ligands [Bruland, 1989; Lohan et al., 2005]. This reduces the bioavailable free Zn<sup>2+</sup> to concentrations < 2 pM by assuming no ligand bound Zn is bioavailable and these concentrations have been shown to limit phytoplankton growth in culture experiments [Brand et al., 1983; Sunda and Huntsman, 1992, 1995; De La Rocha et al., 2000; Saito and Goepfert, 2008]. A Zn concentration of 0.8 pM reduced the activity of carbonic anhydrase in phytoplankton, potentially limiting CO<sub>2</sub> uptake and growth [Morel et al., 1994; Tortell et al., 2000]. Alkaline phosphatase plays an important role in allowing microorganisms to acquire phosphorus from organic compounds [Riegman et al., 2000; Dyhrman and Palenik, 2003]. The activity of alkaline phosphatase in phytoplankton was reduced when grown at 0.4 pM Zn [Shaked et al., 2006]. In diatoms, the uptake of silicate has also been shown to be inhibited by low Zn concentrations [Rueter and Morel, 1981; De La Rocha et al., 2000] with possible changes to community structure as a result [Leblanc et al., 2005]. Diatoms are responsible for the majority of carbon exported from the surface to the deep ocean [Nelson et al., 1995; Tortell et al., 2000]. Therefore a community shift, and/or change in silicification rates, under low Zn conditions may alter the silicate to carbon uptake ratio of the phytoplankton community. This in turn has clear implications for the efficiency of the biological carbon pump.

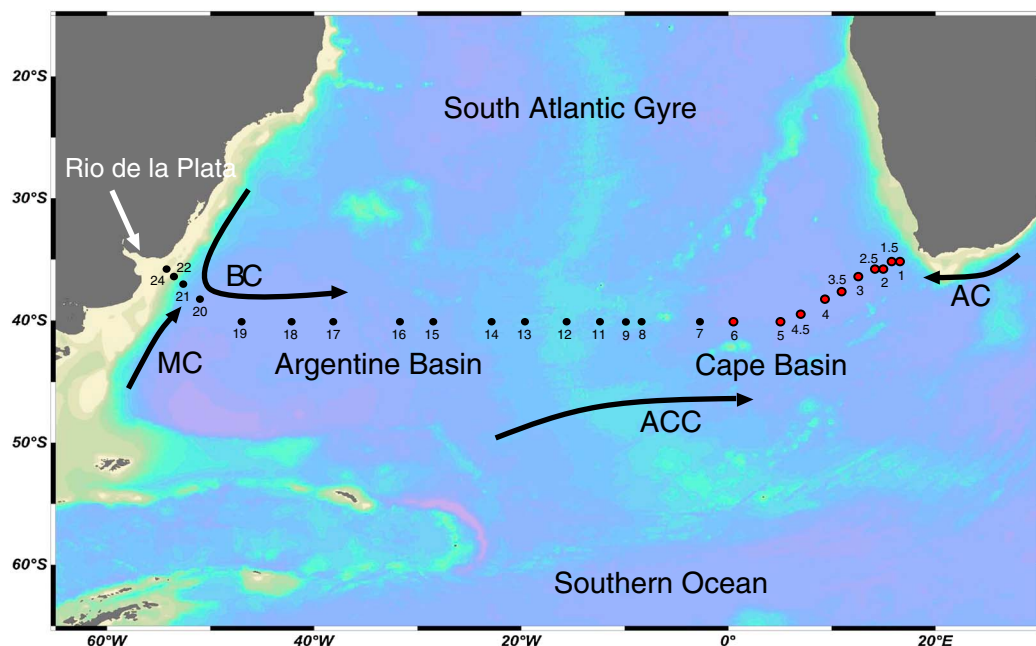


**Figure 1.** The stations sampled for dissolved Zn along section GA10 during two UK GEOTRACES cruises D357 (red circles) and JC068 (black circles). Stations 1, 2, and 3 were reoccupied during JC068.

In contrast to laboratory studies, the few shipboard incubation experiments that have been conducted with natural assemblages showed minimal effects of Zn additions on the bulk phytoplankton community [Crawford *et al.*, 2003; Leblanc *et al.*, 2005; Lohan *et al.*, 2005; Jakuba *et al.*, 2012]. One possible explanation for the lack of observed Zn limitation during field studies is biochemical substitution. Some phytoplankton have a requirement for Zn that can be largely alleviated by either cobalt (Co) or cadmium (Cd) in times of Zn stress [Sunda and Huntsman, 1995; Yee and Morel, 1996; Lee and Morel, 1995]. Furthermore, the evidence for Zn limitation in the oceans may be obscured by the more widespread occurrence of Fe limitation.

What is clear is that our understanding of the impact that dissolved Zn might have on open-ocean primary productivity levels has been hindered by the relative paucity of reliable Zn data. Currently, there are no Zn data for the South Atlantic Ocean, although Croot *et al.* [2011] have reported Zn data from 10 profiles along the Zero Meridian between the Antarctic continent and 46°S. The present study focused on determining the biogeochemical cycle of dissolved Zn along 40°S in the Atlantic Ocean, a region of high productivity, but where there is little understanding of the supply of Zn.

## 2. Methods

### 2.1. Sampling Methods

Seawater samples were collected from 26 stations during two UK GEOTRACES cruises between South Africa and South America (Figure 1). The first cruise (D357) took place from 18 October to 22 November 2010, on board the R.R.S. *Discovery*, whilst the second cruise (JC068) took place from 24 December 2011 to 27 January 2012 on the R.R.S. *James Cook*. For the D357 cruise, only samples collected below 1000 m are presented due to differences in seasonal biological uptake and in the Agulhas current.

All sampling bottles were cleaned according to the procedures detailed in the GEOTRACES sample handling protocols [Cutter *et al.*, 2010]. Seawater samples were collected using a titanium CTD frame fitted with 24, 10 L trace metal clean Teflon-coated OTE (Ocean Test Equipment) samplers deployed on a plasma rope. Upon recovery, the OTE bottles were transferred into a class 1000 clean air container and lightly pressurized (1.7 bar) with high purity compressed air, which was filtered in-line using a 0.2  $\mu\text{m}$  cellulose acetate filter capsule (Sartobran P-300, Sartorius). Samples for dissolved Zn were filtered through 0.8/0.2  $\mu\text{m}$  AcroPak Supor polyethersulfone membrane filter capsules (Pall) into 125 mL low density polyethylene bottles. Each sample was acidified to pH

1.7 (0.024 M) by addition of 12 M hydrochloric acid (HCl, UpA, Romil) under a class 100 laminar flow hood. Vertical profile sampling was augmented by high-resolution underway surface samples. Surface seawater was pumped into the trace metal clean laboratory using a Teflon diaphragm pump (Almatec A-15, Germany) connected by acid-washed braided PVC tubing to a towed “fish” positioned at approximately 2 – 3 m. Underway samples were filtered in-line and acidified as described for samples collected from the titanium sampling system.

## 2.2. Dissolved Zinc Determination

Dissolved Zn analysis was carried out in an overpressurized class 1000 clean air container on-board ship. Dissolved Zn was determined using flow injection with fluorimetric detection (FI-FL), as described by *Nowicki et al.* [1994]. Briefly, the sample was buffered in-line to pH 5.2 with 0.3 M ammonium acetate before being loaded onto a chelating iminodiacetic acid (Toyopearl AF-Chelate 650 M) preconcentration column. The column was rinsed using 0.08 M ammonium acetate to remove the seawater matrix cations before Zn was eluted from the column with 0.08 M HCl (SpA, Romil). The HCl eluent entered the reaction stream where it mixed with a 40  $\mu$ M p-tosyl-8-aminoquinoline (pTAQ; Aldrich) solution containing 2 M ammonium hydroxide and 0.5 M boric acid. The emission of the fluorescent complex was detected by a Shimadzu RF-10Axl fluorimeter with excitation and emission wavelengths set to 377 and 495 nm, respectively.

Zinc concentrations were quantified using the method of standard additions to low-Zn ( $0.08 \pm 0.05$  nM,  $n = 10$ ) seawater. All samples and standards were analyzed in triplicate. The accuracy of the method was assessed by the quantification of Zn in surface water (S) and 1000 m water (D2) collected during the SAFE program [*Johnson et al.*, 2007]. The concentration of Zn measured in the SAFE reference samples during this study yielded values of  $0.060 \pm 0.020$  nM ( $n = 7$ ) for S and  $7.72 \pm 0.09$  nM ( $n = 12$ ) for D2 and were in good agreement with the reported consensus values (S =  $0.064 \pm 0.019$  nM; D2 =  $7.66 \pm 0.28$  nM).

Cadmium is known to also form a fluorescent complex with the reagent pTAQ. The potential interference from this element on the observed Zn signal was therefore investigated using Cd additions to low-Zn seawater. The interference from Cd contributed up to 67% of the Zn fluorescence signal. This is comparable to the 70% reported by *Nowicki et al.* [1994] and higher than the 30% reported by *Gosnell et al.* [2012]. Cadmium concentrations for this transect were estimated using global ocean Cd:PO<sub>4</sub><sup>3-</sup> relationships [*Boyle, 1988*] and Zn concentrations were corrected based on 67% of Cd concentration.

## 2.3. Nutrients, Phytoplankton Pigments, Temperature, and Salinity

The dissolved macronutrients silicate, phosphate, and nitrate (determined as nitrate + nitrite, but referred to as nitrate) were determined in all samples for which Zn was determined. These were determined on-board using an AA III segmented-flow AutoAnalyzer (Bran & Luebbe) following colorimetric procedures [*Woodward and Rees, 2001*]. Clean sampling and analysis procedures were adopted according to international GO-SHIP protocols [*Hydes et al., 2010*]. Salinity, temperature, and depth were measured using a CTD system (Seabird 911+). Dissolved O<sub>2</sub> was determined by a Seabird SBE 43 O<sub>2</sub> sensor. Salinity was calibrated on-board using discrete samples using an Autosol 8400B salinometer (Guildline) whilst dissolved O<sub>2</sub> was calibrated using a photometric automated Winkler titration system [*Carritt and Carpenter, 1966*]. For chlorophyll-*a* analysis, samples were filtered (0.7  $\mu$ m Whatman GF/F) and extracted in 90% acetone overnight [*Holm-Hansen et al., 1965*]. The chlorophyll-*a* extract was measured on a precalibrated (spinach chlorophyll-*a* standard, Sigma) Turner Designs Trilogy fluorimeter. Phytoplankton pigment samples (0.5 – 2 L) were filtered (0.7  $\mu$ m Whatman GF/F), flash frozen in liquid nitrogen and stored at  $-80^{\circ}\text{C}$  prior to analysis using a Thermo HPLC system. The matrix factorization program CHEMTAX was used to interpret the contribution of taxonomic groups to total chlorophyll-*a* [*Mackey et al., 1996*].

## 3. Results

### 3.1. Hydrographic Setting and Macronutrient Distributions

The thermohaline structure of the South Atlantic water column at 40°S is determined largely by water masses that have their origins in the high-latitude regions of the Northern and Southern Hemispheres (Figures 2a and 2b). Here, the cold and fresh Sub-Antarctic Surface Water (SASW) meets the relatively warm and salty Sub-Tropical Surface Water (STSW) of the South Atlantic gyre. The SASW has higher macronutrient

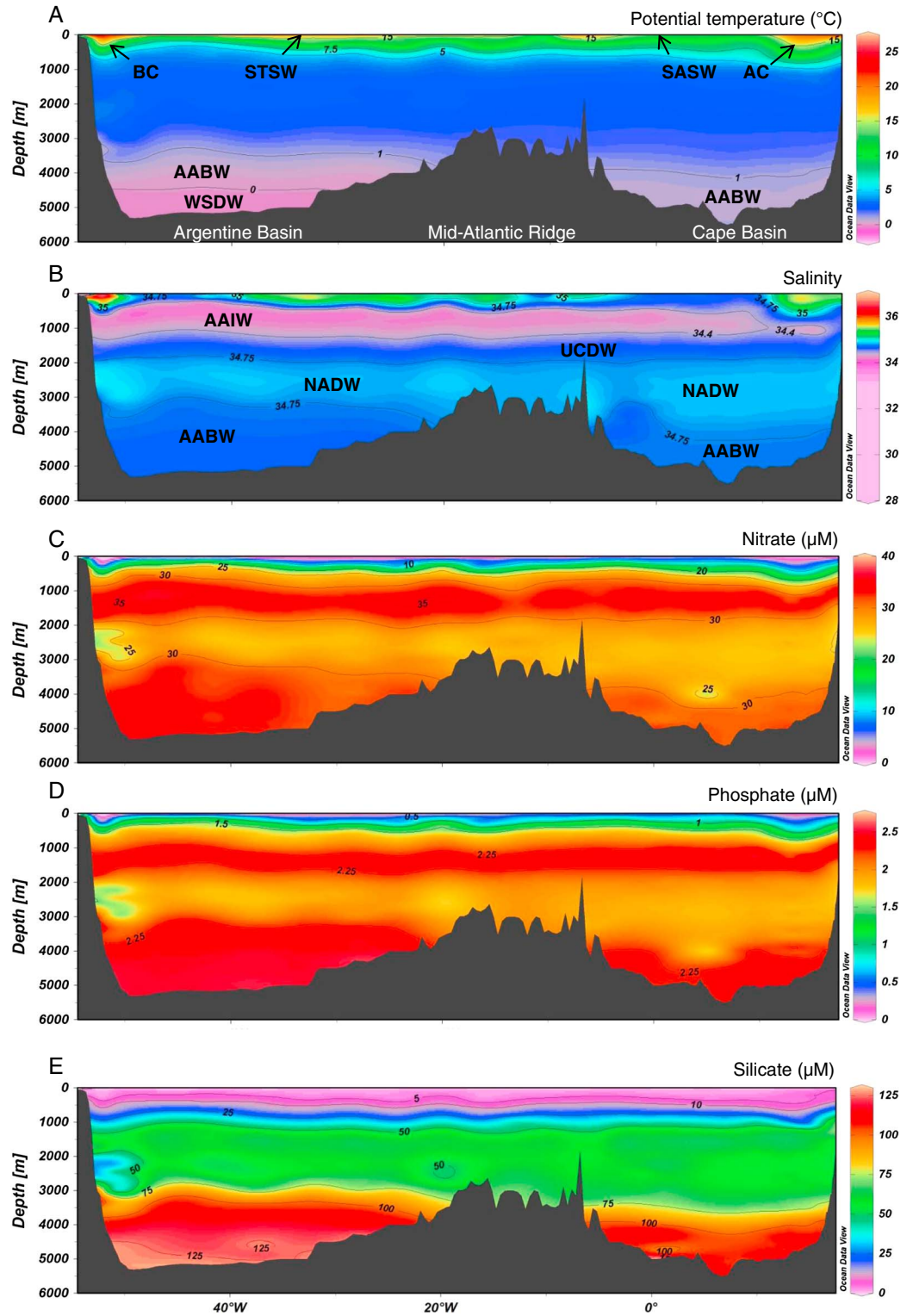


**Figure 2.** Distributions of (A) potential temperature, (B) salinity, (C) nitrate, (D) phosphate, and (E) silicate used to indicate the major water masses at 40°S. Abbreviations in alphabetical order: AABW: Antarctic Bottom Water; AAIW: Antarctic Intermediate Water; AC: Agulhas Current; BC: Brazil Current; NADW: North Atlantic Deep Water; SASW: Sub-Antarctic Surface Water; STSW: Sub-Tropical Surface Water; UCDW: Upper Circumpolar Deep Water; WSDW: Weddell Sea Deep Water.

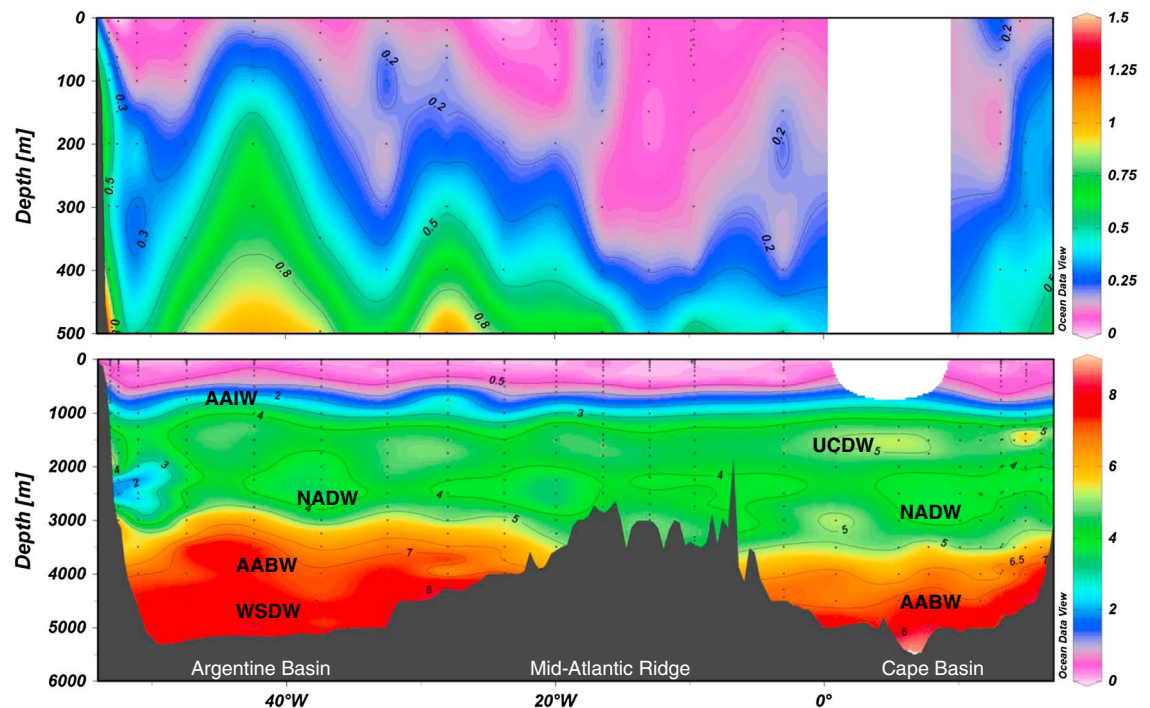


**Figure 3.** Concentrations of dissolved Zn in the upper 500 m (upper plot) and full depth (lower plot). Water mass abbreviations are outlined in Figure 2.

concentrations (nitrate  $> 2.5 \mu\text{M}$  and silicate  $> 1.2 \mu\text{M}$ ) compared with those found within the STSW ( $< 0.1 \mu\text{M}$  nitrate and  $< 1 \mu\text{M}$  silicate) (Figures 2c, 2d, and 2e).

Between South Africa and  $10^\circ\text{E}$ , the leakage of warm ( $\Theta 15\text{--}23^\circ\text{C}$ ) and salty ( $S > 35$ ) waters from the Agulhas Current (AC) was visible at depths to 200 m (Figures 2a and 2b). Nitrate and phosphate concentrations within the AC were low ( $0.02$  and  $0.1 \mu\text{M}$ , respectively) (Figures 2c and 2d). The Brazil Current (BC) was clearly distinguishable by the intrusion of warm ( $\Theta 15\text{--}25^\circ\text{C}$ ) and salty ( $S 35\text{--}37$ ) water to depths of 200 m (Figures 2a and 2b). The macronutrient concentrations in the BC were similar to those found within the STSW. Inshore from the BC at  $54^\circ\text{W}$ , salinity decreased to 28.5 due to freshwater discharge from the Rio de la Plata estuary. High silicate and nitrate concentrations ( $22.2$  and  $13.9 \mu\text{M}$ , respectively) were observed within the vicinity of the low salinity signal.

The two primary intermediate water masses are Antarctic Intermediate Water (AAIW) and Upper Circumpolar Deep Water (UCDW) (Figure 2a). AAIW is thought to be formed by upwelling of circumpolar deep water in either the southeast Pacific Ocean [McCartney, 1977] or in the winter waters of the Bellingshausen Sea [Naveira Garabato et al., 2009] and was identified by its salinity minimum ( $S < 34.4$ ) between 500 and 1250 m. Below this, the UCDW was located at depths between 1250 and 1750 m. Nitrate and phosphate concentrations within these intermediate waters increased with depth to  $\sim 32$  and  $\sim 2.25 \mu\text{M}$ , respectively, at 1750 m (Figures 2c and 2d). It is these intermediate waters, along with the thermocline waters, that constitute the main return branch of the South Atlantic thermohaline overturning circulation [McDonagh and King, 2005].

The abyssal layer was filled by cold, nutrient-rich bottom waters formed around Antarctica, often referred to collectively as Antarctic Bottom Water (AABW) (Figures 2a–e). AABW macronutrient concentrations were the highest observed with nitrate, phosphate, and silicate concentrations of  $\sim 36$ ,  $\sim 2.6$ , and  $\sim 129 \mu\text{M}$ , respectively. The southward flowing NADW was identified by its deep salinity maximum ( $S > 34.75$ ) and reduced macronutrient concentrations (Figures 2a–e).

### 3.2. Distribution of Dissolved Zinc in the South Atlantic

The vertical profiles of dissolved Zn showed nutrient-like distributions with low Zn concentrations ( $0.015 - 0.90 \text{ nM}$ ) in the upper 500 m increasing to values around  $8 \text{ nM}$  in AABW (Figure 3). A slight reduction in Zn ( $0.1 - 1.3 \text{ nM}$ ) was observed within the core of the NADW compared with the Zn-enriched Southern Ocean waters that encompass it.

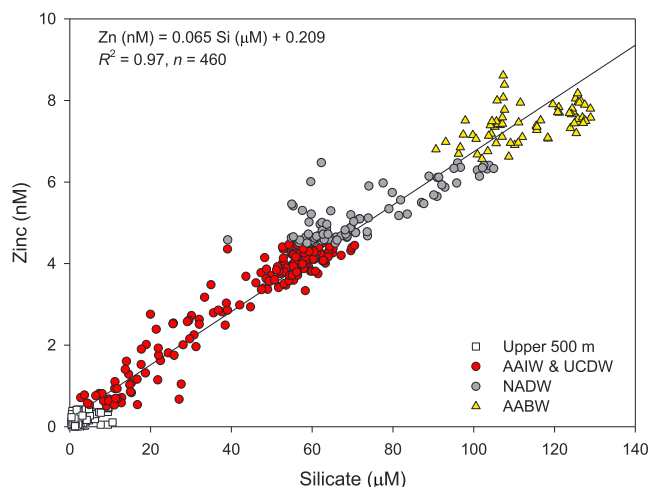


**Figure 4.** Concentrations of dissolved Zn versus dissolved silicate for the complete data set.

The concentrations of Zn in the upper surface layer (10 – 25 m) averaged  $0.13 \pm 0.09$  nM except for stations closest to the South African and South American continents where Zn concentrations of 0.40 and 1.15 nM, respectively, were observed. A subsurface Zn minimum ( $0.090 \pm 0.07$  nM,  $n = 15$ ) was observed at most stations at depths between 25 and 100 m. The Zn minimum was generally located within the vicinity of the chlorophyll-*a* maximum, but no relationship ( $p > 0.05$ ) was observed between Zn and chlorophyll-*a* concentration in the Cape Basin. For the Argentine Basin, a significant negative correlation between Zn and chlorophyll-*a* concentration was observed ( $r^2 = 0.91$ ,  $p < 0.01$ ,  $n = 11$ ).

Zinc concentrations obtained from the underway sampling system (2–5 m) were within the range of the averaged upper 25 m samples from the CTD. The highest Zn concentrations were found on the Uruguayan Shelf (0.70 – 1.25 nM) and coincided with elevated silicate concentrations and a decrease in salinity from 32.6 to 29.4, indicating that this region is influenced by freshwater inputs from the Rio de la Plata.

The stations closest to the South African continent displayed elevated upper surface layer Zn concentrations, averaging  $0.39 \pm 0.01$  nM, whilst surface concentrations for the open-ocean Cape Basin averaged  $0.05 \pm 0.04$  nM. Below the upper surface layer, Zn concentrations increased to  $\sim 0.50$  nM at 500 m, before increasing through the salinity minimum of AAIW to  $\sim 3$  nM at 1000 m. Below the AAIW, Zn was elevated to  $\sim 4$  nM within the UCDW and remained fairly constant throughout the underlying NADW. Below the NADW, the cold and nutrient-rich AABW was channelled between the South African continental slope and the mid-Atlantic ridge, elevating the Zn concentrations to  $> 7$  nM.

The stations closest to the South American continent displayed the highest upper surface layer Zn concentrations (1.25 nM). Zinc concentrations for the open-ocean Argentine Basin averaged  $0.15 \pm 0.10$  nM. The Argentine Basin subsurface minimum of  $0.11 \pm 0.07$  nM was more than double that of the Cape Basin. Unlike the Cape Basin, the Zn concentrations in the Argentine Basin did not increase uniformly to 0.5 nM at 500 m but were quite variable in their distribution, with concentrations between 0.6 and 0.9 nM (Figure 3). The Zn distribution in the intermediate and deep waters of the Argentine Basin was not as longitudinally uniform as those in the east (Figure 3). Higher Zn concentrations were observed at 3000 m in the Argentine Basin compared with the Cape Basin (Figure 3). This is due to the introduction of Weddell Sea Deep Water (WSDW;  $\theta < 0^\circ\text{C}$ , Figure 2a) [Naveira Garabato *et al.*, 2002; Huhn *et al.*, 2008] to the Argentine Basin below 4500 m, which results in the shoaling of AABW. At two stations above the South American continental slope, Zn concentrations as low as 1.7 nM were observed between 1750 and 3000 m (Figure 3), which coincided with reduced potential temperature, salinity, and macronutrient values (Figures 2a–e), indicating the mixing of different water masses.

### 3.3. The Zinc-Silicate Relationship in the South Atlantic

As reported for the ocean environment [Bruland and Franks, 1983; Martin *et al.*, 1990; Lohan *et al.*, 2002; Ellwood, 2008; Croot *et al.*, 2011], the dissolved Zn profile is similar to that of dissolved silicate (Figures 2e and

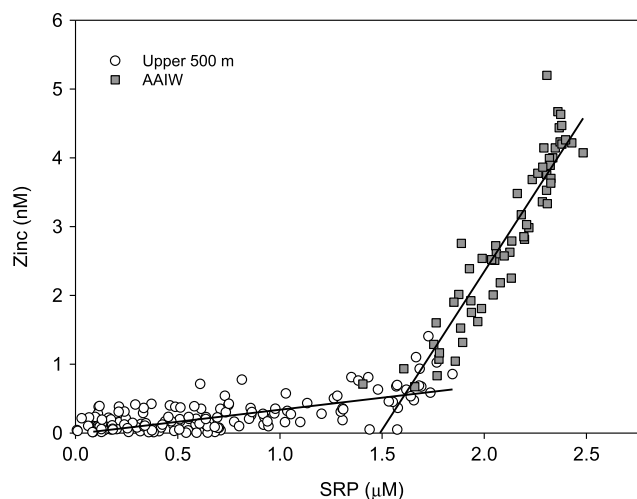


**Figure 5.** Concentrations of dissolved Zn versus soluble reactive phosphorus (SRP) in the upper 500 m and between 500 m and 1250 m (AAIW).

3). Unlike Zn, which decreased to near-zero concentrations at the surface, silicate concentrations at the majority of stations were homogenous within the top ~50 m, suggesting that Zn may become limiting to phytoplankton growth before silicate. Using the complete data set, a significant Zn versus silicate correlation,  $Zn \text{ (nM)} = 0.065 Si \text{ (}\mu\text{M)} + 0.209$  ( $r^2 = 0.97$ ,  $n = 460$ ), was observed (Figure 4).

#### 3.4. The Zinc-Soluble Reactive Phosphorus Relationship in the South Atlantic

Similar to that observed for silicate, a relationship between dissolved Zn and SRP was observed (Figure 5), consistent with biological uptake and vertical export of Zn. The slope of the Zn to SRP ratio reflects the aggregate stoichiometry of biological processes [Saito *et al.*, 2010]. As shown in Figure 5, this relationship has a “kink” at 500 m ( $< 1.5 \mu\text{M PO}_4^{3-}$ ) resulting in a Zn:SRP ratio of  $349 \mu\text{mol mol}^{-1}$ , whilst in the AAIW (500–1250 m) a Zn:SRP ratio of  $4604 \mu\text{mol mol}^{-1}$  was observed.

## 4. Discussion

### 4.1. Zinc in South Atlantic Surface Waters

The concentrations of Zn in the upper 25 m of the open South Atlantic Ocean ( $0.13 \pm 0.09 \text{ nM}$ ) are much lower than the  $0.5 - 0.7 \text{ nM}$  reported for both the open North East Atlantic and Atlantic sector of the Southern Ocean [Nolting *et al.*, 2000; Croot *et al.*, 2011] and are more typical of the concentrations reported for the North East Pacific [Lohan *et al.*, 2002; Jakuba *et al.*, 2012], the Pacific sector of the Southern Ocean [Coale *et al.*, 2003], sub-Antarctic water [Ellwood, 2008], and the Indian Ocean [Gosnell *et al.*, 2012]. Zinc concentrations within the upper 25 m of the central Cape Basin are some of the lowest values reported for the world’s oceans. This is due to a combination of the origins of the surface waters present at  $40^\circ\text{S}$  and the biological removal of Zn. As the SASW waters travel north into the South Atlantic, the concentrations of both Zn and silicate decrease due to the constant export of biogenic particles, including diatom frustules [Löscher, 1999]. The incorporation of Zn and silicate into diatom opal [Ellwood and Hunter, 2000a; Andersen *et al.*, 2011] results in a deeper regeneration cycle than those of nitrate and phosphate [Bruland and Franks, 1983]. The subsurface Zn minimum for the Cape Basin coincided with the chlorophyll-*a* maximum, indicating that uptake by phytoplankton and export from surface waters are important mechanisms for the removal of Zn from the mixed layer. This is consistent with the findings of Löscher [1999] and Croot *et al.* [2011] who also reported low subsurface Zn concentrations in the vicinity of elevated chlorophyll concentrations for the Southern Ocean.

In contrast to the Cape Basin, chlorophyll-*a* concentrations in the upper 25 m of the Argentine Basin were lower ( $\sim 0.2 \text{ mg m}^{-3}$ ) whilst Zn concentrations were slightly higher; hence, phytoplankton growth and productivity may have been primarily limited by the low macronutrient concentrations of the STSW. The slightly elevated Zn in surface waters of the Argentine Basin is not a result of atmospheric sources, which were minimal during this study (R. Chance, 2012, personal communication). A possible source of Zn is the influence

of cross-frontal mixing between the Malvinas current and Brazil Current, which may bring Zn-enriched waters northward as it flows over the Argentine continental margin [Jullion *et al.*, 2010].

Coastal waters were enriched with Zn within the upper 25 m compared with the open ocean. The South African coastal stations had upper surface Zn concentrations similar to those reported for surface waters of the AC in the Indian Ocean [Gosnell *et al.*, 2012]. Reduced macronutrient and chlorophyll-*a* concentrations in the AC prevented the depletion of Zn in these waters. Higher Zn concentrations were observed on the Uruguayan Shelf and coincided with a decrease in salinity and an increase in temperature and macronutrient concentrations, most notably silicate resulting from the discharge of freshwater from the Rio de la Plata estuary.

#### 4.2. Zinc in South Atlantic Deep Waters

The distribution of Zn in the deep waters (> 1750 m) at 40°S is primarily influenced by the inflow of NADW and AABW. The intrusion of NADW is clearly identified by lower Zn (Figure 3) and nitrate (Figure 2c) concentrations between 1750 and 3500 m in the Cape Basin and 1750 and 3000 m in the Argentine Basin. The Zn concentrations observed in the NADW are consistent with the values of 4.2 – 4.5 nM reported for the NADW by Croot *et al.* [2011] for a Southern Ocean station north of the Antarctic Polar Front at 50°S, 0°W.

High Zn concentrations averaging 7.2 nM were observed in the AABW of the Cape Basin below 3000 m (Figure 3). Our data are higher than the values reported by Croot *et al.* [2011] and compare more closely with the values reported by Löscher [1999] for lower circumpolar deep water. Local enrichments in Zn concentration between 8 and 8.6 nM were observed within the deep Cape Basin at depths just above the seafloor, which coincided with elevated silicate concentrations of 107  $\mu\text{M}$ . This suggests that the resuspension of opal-rich sediments may be an important source of Zn and silicate to the water column in this region.

Within the Argentine Basin the introduction of WSDW (Figure 2a) forces AABW to shoal and subsequently Zn concentrations were higher at 3000 m depth in the Argentine Basin (Figure 3). Croot *et al.* [2011] observed no elevation in deep water Zn concentrations associated with the Bouvet Ridge hydrothermal system to the south of our transect. Furthermore, we observed no Zn inputs from the mid-Atlantic Ridge, suggesting that hydrothermal activity is not a significant source of dissolved Zn to the South Atlantic Ocean and Atlantic sector of the Southern Ocean, as reported for Fe [Klunder *et al.*, 2011].

#### 4.3. The Zinc-Silicate Relationship in the South Atlantic

The overall Zn:Si ratio of 65  $\mu\text{mol mol}^{-1}$  observed during this study (Figure 4) is similar to the 77  $\mu\text{mol mol}^{-1}$  reported for the Southern Ocean [Ellwood, 2008] and the 59  $\mu\text{mol mol}^{-1}$  reported for both the Drake Passage [Martin *et al.*, 1990] and Indian Ocean [Gosnell *et al.*, 2012]. The ratio observed in the upper water column (25  $\mu\text{mol mol}^{-1}$ ) is similar to that reported for the highly productive surface waters of the Ross Sea (17  $\mu\text{mol mol}^{-1}$ ) [Fitzwater *et al.*, 2000]. Culture studies have shown that the majority of Zn in diatoms is incorporated into organic material (> 97%), yet the Zn:Si ratio in the opal of diatom frustules is positively correlated with the availability of free  $\text{Zn}^{2+}$  in the growth media [Ellwood and Hunter, 2000a]. The physiological mechanisms that determine why Zn and silicate should be correlated in the oceans are unclear. Initial studies have shown that silicate uptake by diatoms is inhibited by a Zn deficiency [Rueter and Morel, 1981; De La Rocha *et al.*, 2000; Ellwood and Hunter, 2000a]. Recent studies have shown that Zn facilitates the uptake of silicate at low silicate concentrations by its presence in the active center of silicon containing trans-membrane proteins [Grachev *et al.*, 2005]. Danilovtseva *et al.* [2009] suggest that it may be polyamine-Zn complexes within the active centers of these transport proteins that aid the assimilation of silicate from seawater by silicifying organisms. However, Thamtrakoln and Hilderbrand [2008] found no evidence to support the argument that Zn aids silicate transport.

The observed trends in Zn:Si ratios from seawater have been used to estimate the changes in trace metal availability in surface waters [Ellwood and Hunter, 2000b; Hendry and Rickaby, 2008; Andersen *et al.*, 2011]. The ratios of Zn:Cd (where Cd has been estimated from P; Boyle, 1988) have been used as a sensitive paleo-tracer for the glacial-interglacial interactions between NADW and the Southern Ocean derived deep waters [Marchitto *et al.*, 2000]. However, owing to a lack of deep water Zn data, the validation of this hypothesis is dependent on the estimation of bottom water Zn concentrations using a global deep water (>1000 m) Zn-Si relationship ( $\text{Zn} = 0.052[\text{Si}] + 0.79$ ) and measured silicate concentrations [Marchitto *et al.*, 2000]. Our new, large data set suggests that this approach may result in an underestimation of Zn concentrations in

AABW of the South Atlantic and subsequently an underestimation of our understanding of changes in deepwater upwelling and circulation, which are the main sources of glacial/interglacial variations in the surface water  $\text{Zn}^{2+}$  concentrations of the South Atlantic [Ellwood and Hunter, 2000b]. By applying our AABW relationship of  $\text{Zn} = 0.02[\text{Si}] + 5.13$  to the measured silicate values, we estimate a mean AABW Zn concentration of  $7.40 \pm 0.21$  nM compared with the measured concentration of  $7.44 \pm 0.44$  nM. This is higher than the  $6.69 \pm 0.56$  nM estimated by the global deep water relationship of Marchitto *et al.* [2000]. Our data therefore highlight the requirement for more concomitant deep water Zn and silicate data to accurately determine the relationship between present and therefore past ocean Zn biogeochemistry.

#### 4.4. The Biological Control on Zinc Distribution in the South Atlantic

Correlations between Zn and SRP have been reported as evidence for biological uptake and remineralization [Sunda and Huntsman, 1995]. Studies in the North Pacific, the Southern Ocean, and the Ross Sea have shown that the Zn:SRP ratio exhibits a distinct kink in its profile between 20 and 150 m ( $1.2 - 1.5 \mu\text{M PO}_4^{3-}$ ) [Sunda and Huntsman, 1995; Saito *et al.*, 2010; Jakuba *et al.*, 2012]. The Zn:SRP ratio in this study also showed a kink at  $\sim 1.5 \mu\text{M SRP}$  but at a greater depth of  $\sim 500$  m (Figure 5). The relationships found above and below the kink were similar to values from the North Pacific, with a Zn:SRP ratio of  $349 \mu\text{mol mol}^{-1}$  in waters above 500 m and  $4604 \mu\text{mol mol}^{-1}$  in the AAIW that sits immediately below.

An explanation for the apparent kinks in these linear relationships is still under debate due to our limited knowledge of Zn biogeochemistry, hindered by a paucity of Zn data. The mechanisms proposed for this kink include: (1) the excess uptake of Zn by phytoplankton at the base of the euphotic zone followed by export and remineralization of high Zn:SRP particulate material in deeper waters [Saito *et al.*, 2010]. The presence of Zn-binding ligands in excess of the Zn concentration may also contribute to this effect as the free  $\text{Zn}^{2+}$  concentration will decrease concurrently, and (2) the influence of Fe limitation, which decreases P uptake whilst maintaining metal uptake rates, resulting in increased cellular metal:P ratios through a process termed "growth-rate dilution" [Sunda and Huntsman, 2000; Cullen *et al.*, 2003; Cullen, 2006]. Both mechanisms would result in elevated Zn:SRP ratios in phytoplankton that deplete Zn relative to SRP in the upper water column, followed by export and remineralization below the euphotic zone. We propose an additional mechanism, whereby higher Zn concentrations are returned from the Southern Ocean by AAIW and the kink results from the differences in biological utilization of these different water masses.

According to the Redfield theory [Redfield *et al.*, 1963], if phytoplankton are primarily responsible for the relative changes in Zn:SRP ratios then these values reflect the Zn:SRP ratio in phytoplankton responsible for the removal of these elements. The Zn:SRP ratios observed in the South Atlantic can therefore be compared with the trace metal requirements of phytoplankton grown in cultures under growth-rate-limiting conditions [Sunda and Huntsman, 1992, 1995] and subsequently used to interpret the biological impact that Zn concentrations have in this region. Based on analyses of pigment markers, the dominant phytoplankton species within the open South Atlantic Ocean during this study were estimated to be haptophytes (approx. 51% of total chlorophyll-*a*). In contrast, diatoms made up approximately 11% of total chlorophyll-*a*. Our upper 500 m Zn:SRP ratio of  $349 \mu\text{mol mol}^{-1}$  was in excess of the minimum Zn concentration required for optimal growth by the small open-ocean diatom *Thalassiosira oceanica* ( $\sim 110 \mu\text{mol mol}^{-1}$ ) but not the haptophyte *Emiliania huxleyi* ( $\sim 1100 \mu\text{mol mol}^{-1}$ ).

Using the variations in Zn:SRP in this study and the robust relationship between Zn:SRP and free  $\text{Zn}^{2+}$  in phytoplankton [Sunda and Huntsman, 1992, 1995], we estimated free  $\text{Zn}^{2+}$  concentrations of  $0.6 - 80$  pM, which are similar to the sub-Arctic North Pacific [Jakuba *et al.*, 2012] but lower than the Zn-ligand saturated, high Zn surface waters of the Southern Ocean ( $\text{Zn}^{2+} > 100$  pM) [Croot *et al.*, 2011]. At free  $\text{Zn}^{2+}$  concentrations of 1 pM, the growth rate of the haptophytes *E. huxleyi* and *Phaeocystis antarctica* as well as the coastal diatoms *T. pseudonana* and *T. weissflogii* was limited in culture studies [Sunda and Huntsman, 1992, 1995; De La Rocha *et al.*, 2000; Saito and Goepfert, 2008]. These results suggest that the low Zn concentrations in the South Atlantic Ocean may influence phytoplankton species composition by selecting for phytoplankton cells which have a lower cellular requirement for Zn. This is in contrast to the observed phytoplankton distribution, where the highest haptophyte abundance corresponded with the lowest Zn concentrations. The haptophytes *E. huxleyi* and *P. antarctica*, as well as several diatoms, have been shown to substitute Co for Zn and vice versa in growth-limiting culture experiments [Sunda and Huntsman, 1995; Saito and Goepfert, 2008]. There is also evidence for this substitution in oceanic environments [Jakuba *et al.*, 2008] and may be occurring in this region.

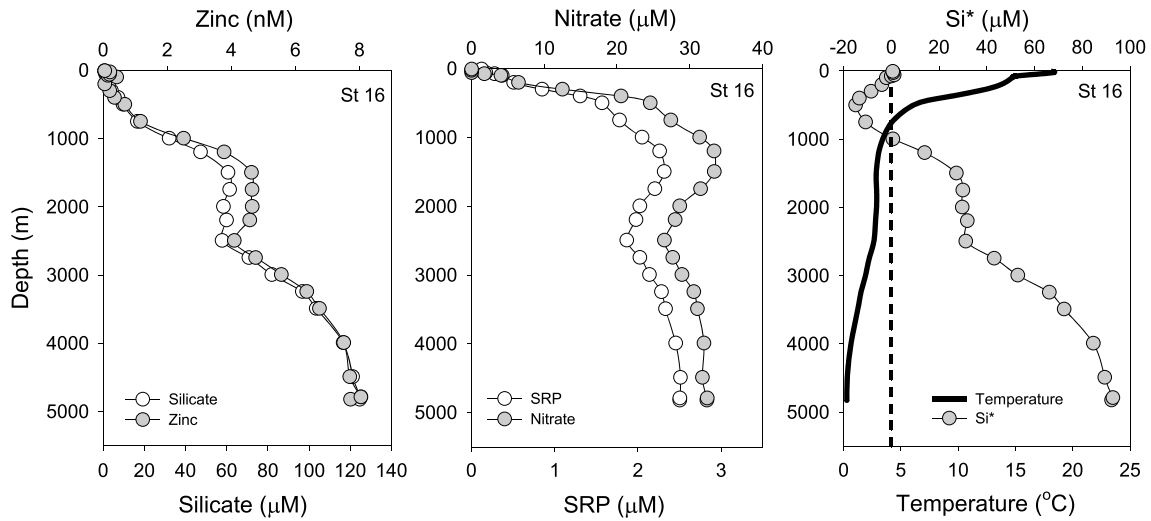


**Figure 6.** Vertical profiles of dissolved Zn, silicate, nitrate, soluble reactive phosphorus (SRP), Si\*, and temperature from station 16 in the Argentine Basin. SAMW is indicated by Si\* < 0 (dashed line).

During our study, a weak but significant relationship ( $r^2 = 0.21$ ,  $p < 0.05$ ,  $n = 21$ ) was observed between the open-ocean Zn concentration and the marker pigment for diatom distribution (total chlorophyll-*a* normalized fucoxanthin). This may be in part due to the low cellular Zn requirement of open-ocean diatom species such as *T. oceanica* [Sunda and Huntsman, 1992, 1995], which is a likely evolutionary adaptation to more oligotrophic and Zn-deplete waters. Only at the lowest Zn concentrations (~ 15 pM) observed for the South Atlantic would the estimated free Zn<sup>2+</sup> concentration (~ 0.6 pM) be potentially growth limiting to *T. oceanica*.

#### 4.5. The Southern Ocean Control on Zinc Distribution in the Upper 500 m

An intriguing result of this study is the low Zn and silicate concentrations within the upper 500 m (Figures 2e and 3). This is in contrast to both nitrate and phosphate (Figures 2c and 2d) whose concentrations increase significantly below 50 m. One explanation for this may be that unlike nitrate and phosphate, Zn and silicate are not being returned to the upper 500 m at 40°S by Southern Ocean mode waters. The Southern Ocean is a critical region for the biological carbon pump, strongly influencing both integrated global export [Sarmiento *et al.*, 2004; Palter *et al.*, 2010] and the overall efficiency of the pump [Sarmiento and Orr, 1991; Marinov *et al.*, 2006].

Sub-Antarctic Mode Water (SAMW) has been identified as the main conduit returning nutrients from the surface waters of the frontal Southern Ocean to the thermocline waters of the Southern Hemisphere [Sarmiento *et al.*, 2004; Palter *et al.*, 2010], accounting for about three quarters of biological production north

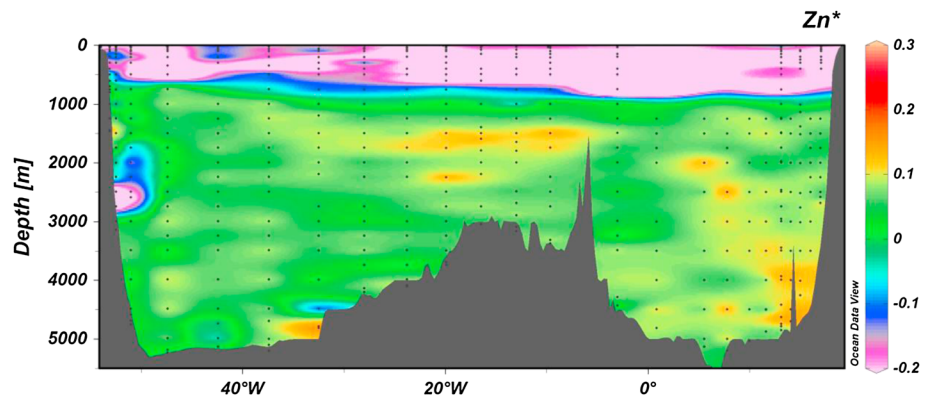


**Figure 7.** The Zn\* tracer indicating the transport of low Zn concentrations from the Southern Ocean to 40°S with SAMW and the upper portion of AAIW (negative Zn\*).

of 30°S [Sarmiento *et al.*, 2004]. One unusual characteristic of SAMW is low Si:NO<sub>3</sub><sup>-</sup> ratios, generally attributed to the preferential removal of silicate by diatoms under Fe limitation [Franck *et al.*, 2000]. Given the high Zn requirement by diatoms for silicate uptake and the strong oceanic Zn:Si relationship, it is reasonable to assume that the removal of silicate in the SAMW formation regions would also result in the removal of Zn from these surface waters as hypothesized by Ellwood [2008] for sub-Antarctic Pacific waters.

In Figure 6, we have utilized the Si\* tracer of SAMW (Si\* = Si(OH) – NO<sub>3</sub><sup>-</sup>), [Sarmiento *et al.*, 2004] to map this water mass at 40°S. Negative Si\* values between 100 and 800 m indicate that this tracer included the upper portion of AAIW, which is formed immediately to the south of SAMW in the Southern Ocean. A new tracer Zn\* (Zn\* = Zn – 0.065 × Si + 0.209), based on our Zn:Si relationship, indicates the transport of negative Zn\* values from the SAMW and upper portion of AAIW (down to ~800 m) at 40°S, and suggests that SAMW and the upper portion of AAIW were not a significant return path for Zn from the Southern Ocean (Figure 7). This tracer has the potential to investigate the transport of low Zn waters from the Southern Ocean to thermocline tropical waters and may explain the low Zn:P in surface waters of the subtropical Atlantic Ocean [Jakuba *et al.*, 2008].

This argument is further strengthened by the kink in the Zn:SRP ratio being observed at 500 m rather than at the shallower depths reported for other oceanographic regions. Below 500 m, our AAIW Zn:SRP ratio of 4604 μmol mol<sup>-1</sup> is slightly higher than the 3800 μmol mol<sup>-1</sup> reported for the AAIW formation region of the Southern Ocean [Croot *et al.*, 2011]. The difference between these ratios may reflect the export of Zn-rich biogenic particles out of SAMW as this water mass travels north and their subsequent remineralization in the underlying AAIW, further reducing the potential for SAMW to return Zn efficiently to the upper thermocline waters of the South Atlantic Ocean.

The Si\* tracer can also be used to provide further insight into the nutrient status of diatoms in the South Atlantic. Diatoms with adequate light and nutrients (including Fe) are reported to contain silicate and nitrate in a mole ratio of about 1:1 [Ragueneau *et al.*, 2000], which requires Si\* ≥ 0 [Sarmiento *et al.*, 2004]. The presence of negative Si\* SAMW at the base of the thermocline at open ocean stations (Figure 6) is associated with a Si:NO<sub>3</sub><sup>-</sup> ratio of ≤ 0.5, suggesting low diatom production. Using our data at 40°S we hypothesize that the potential for low diatom production in this region and most likely throughout the open South Atlantic Ocean may be in-part facilitated by the availability of dissolved Zn, which is maintained at low concentrations by the lack of a significant Southern Ocean return path with SAMW.

## 5. Conclusions

We present dissolved Zn data for 556 discrete samples, the largest Zn data set reported to date. Surface Zn concentrations of 0.015 – 0.39 nM are among the lowest reported for the world's oceans, indicating the absence of a significant source of Zn to these waters and the potential for Zn limitation of phytoplankton growth. Here we suggest, using the Si\* and the new Zn\* tracer, that the low surface Zn concentrations are sustained by the lack of a return path from the Southern Ocean that returns high nitrate and phosphate concentrations to the thermocline waters at this latitude. Despite this, phytoplankton groups with cellular Zn requirements in excess of that available in the surface waters were dominant along the transect suggesting the potential co-substitution of Zn for alternative trace metals. The kink in the Zn-SRP relationship at ~ 500 m is a result of the relative differences in biological utilization between water masses.

### Acknowledgments

The authors gratefully acknowledge the captains and crew of the RSS *Discovery* and *James Cook* for their excellent shipboard support. Our thanks to Bronwyn Wake, Rosie Chance, Christian Schlosser, Jessy Klar, and Maxi Castrillejo for their help with trace metal sampling. This study was supported by a National Environmental Research Council (NERC) grant (NE/H004475/1) to M.C.L. & E.M.S.W. and a NERC Studentship to N.J.W. (NE/G52388X/1).

### References

- Andersen, M. B., D. Vance, C. Archer, R. F. Anderson, M. J. Ellwood, and C. S. Allen (2011), The Zn abundance and isotopic composition of diatom frustules, a proxy for Zn availability in ocean surface seawater, *Earth Planet. Sci. Lett.*, *301*, 137–145.
- Boyle, E. A. (1988), Cadmium: Chemical tracer of deepwater paleoceanography, *Paleoceanography*, *3*, 471–489.
- Brand, L. E., W. G. Sunda, and R. R. L. Guillard (1983), Limitation of marine-phytoplankton reproductive rates by zinc, manganese, and iron, *Limnol. Oceanogr.*, *28*, 1182–1198.
- Bruland, K. W. (1980), Oceanographic distributions of cadmium, zinc, nickel, and copper in the North Pacific, *Earth Planet. Sci. Lett.*, *47*, 176–198.
- Bruland, K. W. (1989), Complexation of zinc by natural organic-ligands in the central North Pacific, *Limnol. Oceanogr.*, *34*, 269–285.
- Bruland, K. W., and R. P. Franks (1983), Mn, Ni, Cu, Zn and Cd in the western North Atlantic, in *Trace Metals in Seawater*, NATO Conference Series IV; Marine Sciences, edited by C. S. Wong *et al.*, pp. 395–414, Plenum, New York.
- Carritt, D. E., and J. H. Carpenter (1966), Comparison and evaluation of currently employed modifications of the Winkler method for determining dissolved oxygen in seawater; a NASCO Report, *J. Mar. Res.*, *24*, 286–319.

- Coale, K. H., X. J. Wang, S. J. Tanner, and K. S. Johnson (2003), Phytoplankton growth and biological response to iron and zinc addition in the Ross Sea and Antarctic Circumpolar Current along 170 degrees W, *Deep Sea Res., Part II*, *50*, 635–653.
- Crawford, D. W., et al. (2003), Influence of zinc and iron enrichments on phytoplankton growth in the northeastern subarctic Pacific, *Limnol. Oceanogr.*, *48*, 1583–1600.
- Croot, P. L., O. Baars, and P. Streu (2011), The distribution of dissolved zinc in the Atlantic sector of the Southern Ocean, *Deep Sea Res., Part II*, *58*, 2707–2719.
- Cullen, J. T. (2006), On the nonlinear relationship between dissolved cadmium and phosphate in the modern global ocean: Could chronic iron limitation of phytoplankton growth cause the kink?, *Limnol. Oceanogr.*, *51*, 1369–1380.
- Cullen, J. T., Z. Chase, K. H. Coale, S. E. Fitzwater, and R. M. Sherrell (2003), Effect of iron limitation on the cadmium to phosphorus ratio of natural phytoplankton assemblages from the Southern Ocean, *Limnol. Oceanogr.*, *48*, 1079–1087.
- Cutter, G., P. Anderssen, L. Codispoti, P. L. Croot, R. Francois, M. C. Lohan, H. Obata, and M. Rutgers van der Leoff (2010), Sampling and Sample-handling Protocols for GEOTRACES Cruises, [geotraces.org](http://geotraces.org).
- Danilovtseva, E., V. Aseyev, M. Karesoja, and V. Annenkov (2009), Sorption of silicic acid from non-saturated aqueous solution by a complex of zinc ions with poly(vinylamine), *Eur. Polym. J.*, *45*, 1391–1396.
- De La Rocha, C. L., D. A. Hutchins, M. A. Brzezinski, and Y. H. Zhang (2000), Effects of iron and zinc deficiency on elemental composition and silica production by diatoms, *Mar. Ecol. Prog. Ser.*, *195*, 71–79, doi:10.3354/Meps195071.
- Dyhrman, S. T., and B. Palenik (2003), Characterization of ectoenzyme activity and phosphate-regulated proteins in the coccolithophorid *Emiliania huxleyi*, *J. Plankton Res.*, *25*, 1215–1225, doi:10.1093/plankt/fbg086.
- Ellwood, M. J. (2008), Wintertime trace metal (Zn, Cu, Ni, Cd, Pb and Co) and nutrient distributions in the Subantarctic Zone between 40–52 degrees S; 155–160 degrees E, *Mar. Chem.*, *112*, 107–117.
- Ellwood, M. J., and K. A. Hunter (2000a), The incorporation of zinc and iron into the frustule of the marine diatom *Thalassiosira pseudonana*, *Limnol. Oceanogr.*, *45*, 1517–1524.
- Ellwood, M. J., and K. A. Hunter (2000b), Variations in the Zn/Si record over the last interglacial glacial transition, *Paleoceanography*, *15*, 506–514, doi:10.1029/1999PA000470.
- Fitzwater, S. E., K. S. Johnson, R. M. Gordon, K. H. Coale, and W. O. Smith (2000), Trace metal concentrations in the Ross Sea and their relationship with nutrients and phytoplankton growth, *Deep Sea Res., Part II*, *47*, 3159–3179.
- Franck, V. M., M. A. Brzezinski, K. H. Coale, and D. M. Nelson (2000), Iron and silicic acid concentrations regulate Si uptake north and south of the Polar Frontal Zone in the Pacific Sector of the Southern Ocean, *Deep Sea Res., Part II*, *47*, 3315–3338.
- Gosnell, K. J., W. M. Landing, and A. Milne (2012), Fluorometric detection of total dissolved zinc in the southern Indian Ocean, *Mar. Chem.*, *132*, 68–76.
- Grachev, M. A., T. A. Sherbakova, Y. A. Masyukova, and Y. V. Likhoshway (2005), A potential zinc-binding motif in silicic acid transport proteins of diatoms, *Diatom Res.*, *20*, 409–411.
- Hendry, K. R., and E. M. Rickaby (2008), Opal (Zn/Si) ratios as a nearshore geochemical proxy in coastal Antarctica, *Paleoceanography*, *23*, PA2218, doi:10.1029/2007PA001576.
- Holm-Hansen, O., C. J. Lorenzen, and J. D. H. Holmes (1965), Fluorometric determination of chlorophyll, *J. Const. Int. Explor. Mer.*, *30*, 3–15.
- Huhn, O., H. H. Hellmer, M. Rhein, C. Rodehacke, W. Roether, M. P. Schodlok, and M. Schroder (2008), Evidence of deep- and bottom-water formation in the western Weddell Sea, *Deep Sea Res., Part II*, *55*, 1098–1116.
- Hydes, D. J., et al. (2010), *The GO-SHIP Repeat Hydrography Manual: A Collection of Expert Reports and Guidelines*, IOCCP Report No. 14, ICPO Publication Series No. 134, Version 1.
- Jakuba, R. W., J. W. Moffett, and S. T. Dyhrman (2008), Evidence for the linked biogeochemical cycling of zinc, cobalt, and phosphorus in the western North Atlantic Ocean, *Global Biogeochem. Cycle*, *22*, GB4012, doi:10.1029/2007GB003119.
- Jakuba, R. W., M. A. Saito, J. W. Moffett, and Y. Xu (2012), Dissolved zinc in the subarctic North Pacific and Bering Sea: Its distribution, speciation, and importance to primary producers, *Global Biogeochem. Cycle*, *26*, GB2015, doi:10.1029/2010GB004004.
- Johnson, K. S., et al. (2007), Developing standards for dissolved iron in seawater, *Eos Trans. AGU*, *88*, 131–132, doi:10.1029/2007EO110003.
- Jullion, L., H. J. Heywood, A. C. Naveira Garabato, and D. P. Stevens (2010), Circulation and water mass modification in the Brazil-Malvinas Confluence, *J. Phys. Oceanogr.*, *40*, 845–868.
- Klunder, M. B., P. Laan, R. Middag, H. J. W. De Baar, and J. C. Ooijen (2011), Dissolved iron in the Southern Ocean (Atlantic sector), *Deep Sea Res., Part II*, *58*, 2678–2694.
- Leblanc, K., C. E. Hare, P. W. Boyd, K. W. Bruland, B. Sohst, S. Pickmere, M. C. Lohan, K. Buck, M. Ellwood, and D. A. Hutchins (2005), Fe and Zn effects on the Si cycle and diatom community structure in two contrasting high and low-silicate HNLC areas, *Deep Sea Res., Part I*, *52*, 1842–1864, doi:10.1016/j.dsr.2005.06.005.
- Lee, J. G., and F. M. M. Morel (1995), Replacement of zinc by cadmium in marine-phytoplankton, *Mar. Ecol. Prog. Ser.*, *127*, 305–309, doi:10.3354/Meps127305.
- Lohan, M. C., P. J. Statham, and D. W. Crawford (2002), Total dissolved zinc in the upper water column of the subarctic North East Pacific, *Deep Sea Res., Part II*, *49*, 5793–5808.
- Lohan, M. C., D. W. Crawford, D. A. Purdie, and P. J. Statham (2005), Iron and zinc enrichments in the northeastern subarctic Pacific: Ligand production and zinc availability in response to phytoplankton growth, *Limnol. Oceanogr.*, *50*, 1427–1437.
- Löscher, B. M. (1999), Relationships among Ni, Cu, Zn and major nutrients in the Southern Ocean, *Mar. Chem.*, *67*, 67–102.
- Mackey, M. D., D. J. Mackey, H. W. Higgins, and S. W. Wright (1996), CHEMTAX - a program for estimating class abundances from chemical markers: application to HPLC measurements of phytoplankton, *Mar. Ecol. Prog. Ser.*, *144*, 265–283.
- Marchitto, T. M., W. B. Curry, and D. W. Oppo (2000), Zinc concentrations in benthic foraminifera reflect seawater chemistry, *Paleoceanography*, *15*(3), 299–306, doi:10.1029/1999PA000420.
- Marinov, I., A. Gnanadesikan, J. R. Toggweiler, and J. L. Sarmiento (2006), The Southern Ocean biogeochemical divide, *Nature*, *441*, 964–967.
- Martin, J. H., R. M. Gordon, and S. E. Fitzwater (1990), Iron in Antarctic Waters, *Nature*, *345*, 156–158, doi:10.1038/345156a0.
- McCartney, M. S. (1977), Subantarctic Mode Water, *Deep Sea Res.*, *24*, 103–119.
- McDonagh, E. L., and B. A. King (2005), Oceanic fluxes in the South Atlantic, *J. Phys. Oceanogr.*, *35*, 109–122, doi:10.1175/Jpo-2666.1.
- Morel, F. M. M., and N. M. Price (2003), The biogeochemical cycles of trace metals in the oceans, *Science*, *300*, 944–947, doi:10.1126/science.1083545.
- Morel, F. M. M., J. R. Reinfeldt, S. B. Roberts, C. P. Chamberlain, J. G. Lee, and D. Yee (1994), Zinc and carbon co-limitation of marine-phytoplankton, *Nature*, *369*, 740–742, doi:10.1038/369740a0.
- Naveira Garabato, A. C., E. L. McDonagh, D. P. Stevens, K. J. Heywood, and R. J. Sanders (2002), On the export of Antarctic Bottom water from the Weddell Sea, *Deep Sea Res., Part II*, *49*, 4715–4742.

- Naveira Garabato, A. C., L. Jullion, D. P. Stevens, K. J. Heywood, and B. A. King (2009), Variability of Subantarctic Mode Water and Antarctic Intermediate Water in the Drake Passage during the late-twentieth and early-twenty-first centuries, *J. Clim.*, *22*(13), 3661–3688, doi:10.1175/2009jcli2621.1.
- Nelson, D. M., P. Treguer, M. A. Brzezinski, A. Leynaert, and B. Queguiner (1995), Production and dissolution of biogenic silica in the ocean - revised global estimates, comparison with regional data and relationship to biogenic sedimentation, *Global Biogeochem. Cycle*, *9*, 359–372, doi:10.1029/95GB01070.
- Nolting, R. F., M. Heijne, J. T. M. de Jong, K. R. Timmermans, and H. J. W. de Baar (2000), The determination and distribution of Zn in surface water samples collected in the northeast Atlantic Ocean, *J. Environ. Monit.*, *2*, 534–538.
- Nowicki, J. L., K. S. Johnson, K. H. Coale, V. A. Elrod, and S. H. Lieberman (1994), Determination of zinc in seawater using flow-injection analysis with fluorometric detection, *Anal. Chem.*, *66*, 2732–2738.
- Palter, J. B., J. L. Sarmiento, A. Gnanadesikan, J. Simeon, and R. D. Slater (2010), Fuelling export production: nutrient return pathways from the deep ocean and their dependence on the Meridional Overturning Circulation, *Biogeosciences*, *7*, 3549–3568, doi:10.5194/bg-7-3549-2010.
- Ragueneau, O., et al. (2000), A review of the Si cycle in the modern ocean: recent progress and missing gaps in the application of biogenic opal as a paleoproductivity proxy, *Global Planet. Change*, *26*, 317–365.
- Redfield, A. C., B. H. Ketchum, and F. A. Richards (1963), The influence of organisms on the composition of seawater, in *The composition of seawater*. *The Sea*, edited by M. N. Hill, pp. 26–27, Wiley, New York.
- Riegman, R., W. Stolte, A. A. M. Noordeloos, and D. Slezak (2000), Nutrient uptake, and alkaline phosphate (EC 3: 1: 3: 1) activity of *Emiliania huxleyi* (Prymnesiophyceae) during growth under N and P limitation in continuous cultures, *J. Phycol.*, *36*, 87–96.
- Rueter, J. G., and F. M. M. Morel (1981), The interaction between zinc-deficiency and copper toxicity as it affects the silicic-acid uptake mechanisms in *Thalassiosira pseudonana*, *Limnol. Oceanogr.*, *26*, 67–73.
- Saito, M. A., and T. J. Goepfert (2008), Zinc-cobalt colimitation of *Phaeocystis antarctica*, *Limnol. Oceanogr.*, *53*, 266–275, doi:10.4319/lo.2008.53.1.0266.
- Saito, M. A., T. J. Goepfert, A. E. Noble, E. M. Bertrand, P. N. Sedwick, and G. R. DiTullio (2010), A seasonal study of dissolved cobalt in the Ross Sea, Antarctica: micronutrient behavior, absence of scavenging, and relationships with Zn, Cd, and P, *Biogeosciences*, *7*, 4059–4082, doi:10.5194/bg-7-4059-2010.
- Sarmiento, J. L., and J. C. Orr (1991), Three-dimensional simulations of the impact of the Southern Ocean nutrients depletion on atmospheric CO<sub>2</sub> and ocean chemistry, *Limnol. Oceanogr.*, *36*, 1928–1950.
- Sarmiento, J. L., N. Gruber, M. A. Brzezinski, and J. P. Dunne (2004), High-latitude controls of thermocline nutrients and low latitude biological productivity, *Nature*, *427*, 56–60.
- Shaked, Y., Y. Xu, K. Leblanc, and F. M. M. Morel (2006), Zinc availability and alkaline phosphatase activity in *Emiliania huxleyi*: Implications for Zn-P co-limitation in the ocean, *Limnol. Oceanogr.*, *51*, 299–309.
- Sunda, W. G., and S. A. Huntsman (1992), Feedback interactions between zinc and phytoplankton in seawater, *Limnol. Oceanogr.*, *37*, 25–40.
- Sunda, W. G., and S. A. Huntsman (1995), Cobalt and zinc interreplacement in marine phytoplankton: Biological and geochemical implications, *Limnol. Oceanogr.*, *40*, 1404–1417.
- Sunda, W. G., and S. A. Huntsman (2000), Effect of Zn, Mn, and Fe on Cd accumulation in phytoplankton: Implications for oceanic Cd cycling, *Limnol. Oceanogr.*, *45*, 1501–1516.
- Thamatrakoln, K., and M. Hilderbrand (2008), Silicon uptake in diatoms revisited: a model for saturable and nonsaturable uptake kinetics and the role of silicon transporters, *Plant Physiol.*, *146*, 1397–1407.
- Tortell, P. D., G. H. Rau, and F. M. M. Morel (2000), Inorganic carbon acquisition in coastal Pacific phytoplankton communities, *Limnol. Oceanogr.*, *45*, 1485–1500.
- Vallee, B. L., and D. S. Auld (1990), Zinc coordination, function, and structure of zinc enzymes and other proteins, *Biochemistry*, *29*, 5647–5659.
- Woodward, E. M. S., and A. P. Rees (2001), Nutrient distributions in an anticyclonic eddy in the northeast Atlantic Ocean, with reference to nanomolar ammonium concentrations, *Deep Sea Res., Part II*, *48*, 775–793, doi:10.1016/S0967-0645(00)00097-7.
- Yee, D., and F. M. M. Morel (1996), In vivo substitution of zinc by cobalt in carbonic anhydrase of a marine diatom, *Limnol. Oceanogr.*, *41*, 573–577.